SPIRAL–VORTEX STRUCTURE IN THE GASEOUS DISKS OF GALAXIES

A.M. Fridman, O.V. Khoruzhii, V.V. Lyakhovich and V.S. Avedisova
Institute of Astronomy of the Russian Academy of Science, 48, Pyatnitskaya St., Moscow, 109017, Russia

O.K. Sil'chenko, A.V. Zasov and A.S. Rastorguev
Sternberg Astronomical Institute, Moscow State University, University prospect, 13, Moscow, 119899, Russia

V.L. Afanas'iev and S.N. Dodonov
Special Astrophysical Observatory of the Russian Academy of Sciences, Zelenchukskaya, 377140, Russia

and

J. Boulesteix
Observatoire de Marseille, Place le Verrier, F-13248, Marseille, Cedex 04, France

Abstract. General ideas, as well as experimental and theoretical efforts concerning the prediction and discovery of new structures in the disks of spiral galaxies — giant anticyclones – are reviewed. A crucial point is the development of a new method to restore the full vector velocity field of the galactic gas from the line-of-sight velocity field. This method can be used to get self-consistent solutions for the following problems: 1) determination of non-circular velocities associated with spiral–vortex structure; 2) determination of fundamental parameters of this structure: pattern speed, corotation radius, location of giant anticyclones; 3) refinement of galactic rotation curves taking into account regular non-circular motion in the spiral density wave, which makes it possible to build more accurate models of the mass distribution in the galaxy; 4) refinement of parameters of the rotating gaseous disk: inclination angle, center of rotation and position angle of the major dynamical axis, systematic velocity. The method is demonstrated using the restoration of the velocity field of the galaxy NGC 157 as an example. Results for this and some other spiral galaxies suggest that giant anticyclones are a universal property of galaxies with grand design structure.

1 Introduction

The purpose of this work is to show that spiral arms of galaxies, which have been studied for over one and a half centuries since they were first described in 1845 by Lord Rosse, are always accompanied by giant vortices forming part of the common spiral–vortex structure. While spiral arms are visible as regions of enhanced brightness in galactic disks, giant vortices are features of velocity field of a galaxy, and, as a rule, are located between spiral arms in regions of reduced gas surface density. Because they are highly attractive and expressive in shape, spirals decorate the covers of numerous books on astronomy; however they can tell us only a little about the dynamical processes responsible for their formation. In contrast, the giant vortices that are tightly connected with spiral structure are

Astrophysics and Space Science **252**: 115–131, 1997.

carriers of basic dynamic information about the galactic disk. First, the centers of vortices are located near the corotation circle, where the azimuthal rotation velocities of the spiral pattern and disk coincide (Nezlin et al. 1986, Lyakhovich et al. 1996). The pattern speed as a crucial parameter for various theories of spiral structure is a subject of long-standing controversies. The location of the vortex centers relative to spiral arms together with the rotation curve of the disk near the corotation radius indicate whether the mechanism generating the structure is gravitational or hydrodynamic. It is impossible to make such deductions based only on the shape of spiral arms (Lyakhovich et al. 1996).

2 Qualitative picture of anticyclone formation and early evidence for these structures

In the laboratory frame of reference, the angular rotation velocity of a disk $\Omega_d(r)$ decreases with radius (Fig. 1a). Since the spiral structure has a wave nature, it rotates with constant angular velocity Ω_{ph} – const. The intersection of the graphs of the functions $\Omega_d(r)$ and Ω_{ph} = const corresponds to the corotation radius r_c. An observer in a frame rotating with the disk at $r = r_c$ finds the spiral arms to be fixed (stationary). In this case, the parts of the disk inside the circle $r = r_c$ rotate faster than the spiral arms (sign " + " in Fig. 1b), and the parts outside this circle lag behind.

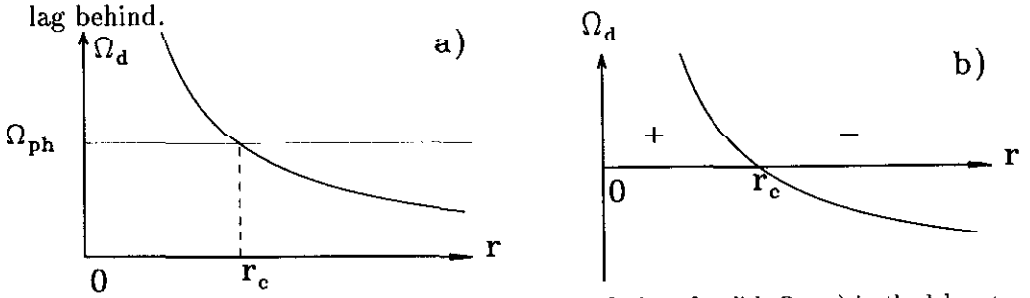

Fig. 1. Radial dependence of the angular rotation velocity of a disk Ω_d: a) in the laboratory reference frame, where Ω_{ph} is the phase velocity of the spiral density wave, b) in a frame rotating with Ω_{ph}. In the latter case, the disk is stationary at the corotation radius r_c. The "+" and "-" signs in Fig. 1b show that the direction of the disk rotation changes sign at the corotation radius.

Thus, in the absence of an instability in the vicinity of the corotation circle, the spiral arms are motionless, so that their surface density and velocities do not change with time:

$$\sigma(r,\varphi) = \sigma_0(r) + \sigma_1(r,\varphi) = \sigma_0(r) + \tilde{\sigma}(r)\cos(2\varphi - F_\sigma)\,, \tag{1}$$

$$v_r(r,\varphi) = v_{1r}(r,\varphi) = \tilde{v}_r(r)\cos(2\varphi - F_r)\,, \tag{2}$$

$$v_\varphi(r,\varphi) = v_{0\varphi}(r) + v_{1\varphi}(r,\varphi) = v_{0\varphi} + \tilde{v}_\varphi(r)\cos(2\varphi - F_\varphi)\,. \tag{3}$$

Here, the indices "0" and "1" designate stationary and perturbed parameters of the disk respectively, the amplitudes of the perturbations are marked by a tilde,

and the F's are the corresponding phases. As an example, we consider the two-armed spiral structure denoted by the value 2φ in the expression for the total phases of the perturbed functions.

According to (1), the perturbed surface density $\sigma_1(r, \varphi)$ at a given r changes sign with azimuth four times (twice the number of spiral arms). Accordingly, both velocity components $v_{1r}(r, \varphi)$ and $v_{1\varphi}(r, \varphi)$ also change sign with azimuth four times. As a result, it is natural to find two anticyclonic vortices in the vicinity of the corotation circle (Fig. 2).

The qualitative picture of anticyclone formation in galactic disks sketched above is based only on the wave nature of spiral arms. It must be universal and independent of either the disk composition (gaseous or stellar) or the nature of the mechanism generating the spiral wave (gravitational or hydrodynamical)[1].

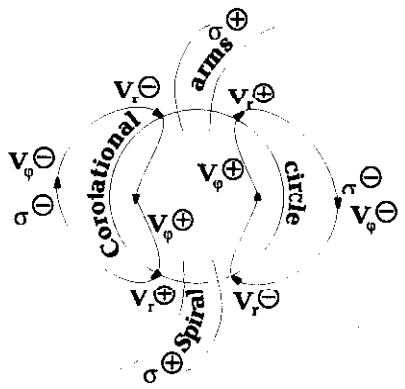

Fig. 2. Scheme for the formation of two anticyclones in the neighbourhood of the corotation circle in the frame of reference rotating with the two-arm spiral pattern. The sign of the density perturbations changes four times along the azimuth angle. The radial velocity behaves in a similar manner. As a result, the velocity field near the corotation radius has the form of two anticyclones.

As shown earlier by Fridman (see Fridman 1990 and references therein), the equations describing the dynamics of a rotating gaseous disk are identical to those for rotating shallow water. This makes it possible to use laboratory experiments to model dynamical processes in galactic gaseous disks. Setups using a rotating shallow water layer with the shape of a "rotation curve" resembling the rotation curve of a galactic disk were built at the Kurchatov Institute Kurchatov Institute (Morozov et al. 1984, 1985; Fridman et al. 1985). Experiments carried out with these setups have demonstrated the formation of spiral structure with inter-arm anticyclones (Nezlin et al. 1986).

This discovery of anticyclones between spiral arms in experiments with rotating shallow water stimulated the search for similar structures in spiral galaxies. The first galaxy where such structures were found was Mrk 1040 (Afanas'iev and Fridman 1993). The residual velocities field in the gaseous disk of Mrk 1040 was

[1] The location of anticyclones relative to the spiral arms depends on the parameters of the system in the corotation region and the mechanism of wave generation (see Lyakhovich et al. 1996).

obtained by subtracting the azimuthally symmetric component of the rotation curve from the line-of-sight velocity field. The structure of the residual velocities (Fig.3 in Afanas'iev and Fridman 1993) showed the presence of two symmetrically located anticyclonic vortices, whose general appearance was in a good agreement with the anticyclonic vortices expected based on the laboratory simulations in shallow water (Nezlin et al. 1986). The observed size of the anticyclones in Mrk 1040 is about 4 kpc, and the velocity amplitude (in projection) is about 25 km/s.

3 Are there giant anticyclones near the solar circle?

The well-known velocity depression as large as 20–30 km/s in the rotation curve of the Galaxy in the solar neighbourhood suggests that there might be an anticyclone in this region (Fridman 1994). The reconstruction of the two dimensional vector velocity field using the line-of sight velocity data for 312 star-forming regions (H II regions, Avedisova 1997) has shown that the velocities of gas clouds within 3–4 kpc from the Sun are consistent with the existence of an anticyclone, whose center is located near the solar orbit between the main spiral arms (Fridman et al. 1996).

We tried to check whether young stellar populations would also trace the anticyclonic structure of gas in the solar neighbourhood. Our sample (Rastorguev 1997, Gluskova et al. 1997) includes: 256 classical cepheids pulsating in fundamental mode; 106 young open clusters with $t \leq 10^8$y, 99 K–M supergiants taken from the list of White & Wing (1978), and 316 molecular clouds (Avedisova 1997). Restoration of the two-dimensional vector velocity field based on the line-of-sight velocity data for young stellar objects has shown that they follow the behavior of the velocities of gaseous clouds, forming an anticyclone (Fig. 3).

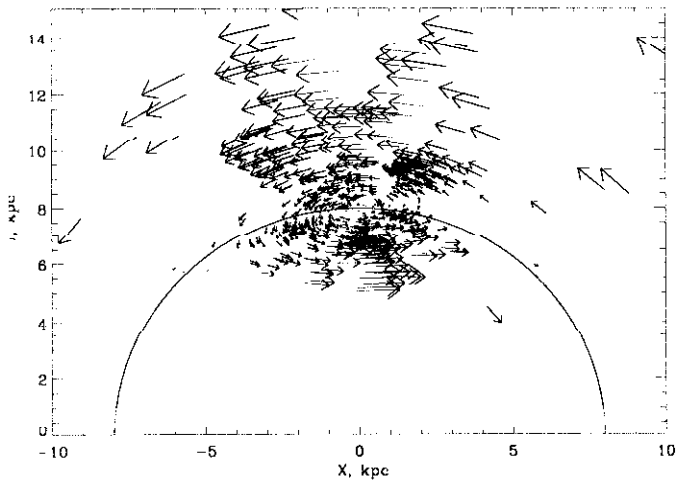

Fig. 3. Restored two-dimensional velocity field of the sample of 461 stellar objects and 316 molecular clouds in a reference frame rotating with the angular velocity of the Local Standard of Rest. The Sun is at the point (0,8).

4 Some remarks

The discovery of the previously predicted anticyclones in the gaseous disk of Mrk 1040 and in the vicinity of the Sun in our Galaxy was rather natural. In both cases, the rotation curve of the gaseous disk has a depression at some radius. The presence of minima in the observed rotation curve can indicate either peculiarity of the equilibrium curve, which can generate hydrodynamical instability, or the existence of local non-circular motions of gas distorting the observed curve. The former case was modeled in the laboratory experiments noted above, in which anticyclonic vortices were discovered, and can result in the simultaneous excitation of spiral arms and vortex structures in the velocity field.

It is rather difficult to detect a velocity kink with an amplitude $\Delta v/v < 10$ % using traditional methods for deriving rotation curves in spiral galaxies from the long slit observations (Afanas'iev et al. 1988). However, the amplitude of the velocity extremum corresponding to the anticyclone in the solar neighbourhood has just this order of magnitude ($\Delta v/v \simeq 10$ %). It is unlikely that a similar decrease of the rotation velocity could be measured reliably in other spiral galaxies. Note also that the velocity kink in the rotation curve of Mrk 1040 in the region where the anticyclones are located is abnormally sharp (which is the extreme case for spiral galaxies), so that the necessary condition for the generation of strong hydrodynamical instabilities is fulfilled. Thus, both of the vortex structures described above correspond to objects that are peculiar in some sense.

On the other hand, the simple arguments given above suggest that anticyclones may exist in all spiral galaxies if their spiral arms are density waves. If these density waves are caused by gravitational instability (Lindblad 1941, Lin & Shu 1964, 1966), then theoretical estimates of the velocity depression $\Delta v/v$ due to noncircular motion near the anticyclone typically lead to values of about 10 %. Hence, the long-slit method of determining rotation curves is not likely to be useful for detecting vortices. It is therefore necessary to develop a new, accurate method for restoring the velocity field from the observed line-of-sight velocities, taking into account the wave oscillations of the gas. In addition, since the centers of the anticyclones lie near the corotation circle (Contopoulos 1978, Nezlin et al. 1986, Lyakhovich et al. 1996), this method should allow determination of the position of the corotation resonance directly from observations. We will show below that this also enables us to reveal vertical gas oscillations, which is important in analyses of the three-dimensional structure of the disk or in investigations of the bending instability (Fridman and Polyachenko 1984). In general, this new method may make it possible to paint a dynamical portrait of a spiral galaxy.

It is clear that restoration of the total (three-dimensional) vector velocity field of the gas in a galaxy from the observed (one–component) field of the line-of-sight velocities is, in general, impossible without making some assumptions. These assumptions should have a rather general character, and should be in agreement with our understanding of the nature of spiral galaxies.

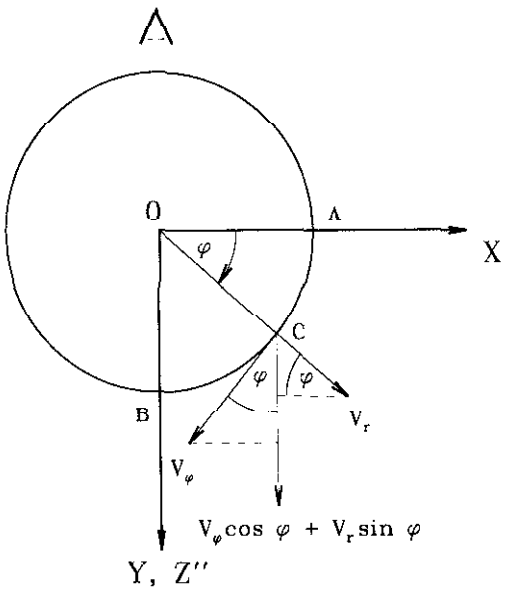

Fig. 4. The relation between line-of-sight velocity and components of the vector velocity field of a gaseous galactic disk.

First, we will show that if we ignore the wave nature and total number of spiral arms, it is fundamentally impossible to restore the total velocity field. Let i be the inclination angle of the galaxy (the angle between the planes of the disk and the sky), and let us measure the line-of-sight velocity of some gaseous cloud C. Generally speaking, the cloud velocity has three components: V_r, V_φ and V_z. First, let us consider the special case $i = \pi/2$. Then, as can easily be seen from Fig. 4, the line-of-sight velocity in the reference frame of the galaxy is $V_r \sin\varphi + V_\varphi \cos\varphi$. In this particular case, the V_z component lies in the plane of the sky, and, as a result, does not contribute to the line-of-sight velocity. With an arbitrary inclination angle i, this contribution will be $V_z \cos i$, and the contributions of V_r and V_φ will diminish: $(V_r \sin\varphi + V_\varphi \cos\varphi) \sin i$. Thus, in the general case, the observed line of sight velocity is

$$V^{obs} = V_s + V_r \sin\varphi \sin i + V_\varphi \cos\varphi \sin i + V_z \cos i, \qquad (4)$$

where V_s is the systemic velocity of the center of mass of the galaxy. V^{obs}, V_s, V_r, V_φ, and V_z characterize the state of the velocity field at the observation time, and so are functions of the galactocentric radius R and azimuth φ, but do not depend on the time t.

The relation (4) is the only that can be deduced between the line-of-sight velocity field and the components of the vector velocity field of a gaseous disk without restricting the generality of the problem. Measurements of line-of-sight velocity

for each pixel give us a set of N_{max} data, where N_{max} is the total number of pixels (with independent estimates of V^{obs}) in the galaxy image. These data can be directly attributed to the measured coordinates in the sky plane (x', y'), which are related to the galactocentric coordinates (R, φ) via the inclination angle i, position angle of the major dynamical axis of the galaxy PA, and the coordinates of the galactic center (x_0, y_0). Consequently, conditions (4) relate the N_{max} measured values of V^{obs} with $(3\,N_{max} + 5)$ unknowns: i, α, x_0, y_0, V_s, V_r, V_φ, and V_z. As a result, direct determination of the velocity field of a gaseous disk in the general case requires $(2\,N_{max} + 5)$ additional conditions. As N_{max} is typically of the order of many thousands, direct restoration of the full velocity field is hopeless.

5 A method for restoring the full vector velocity field from the line-of-sight velocity field

Let us frame the question as follows. Suppose we wish to determine the velocity field in the gaseous disk of a spiral galaxy at the time when its spiral arms have just begun to form. If it is an "m"-armed galaxy, it follows that from the very beginning, the growth of the amplitude of the density wave is the largest for azimuthal number "m", compared to that for other azimuthal numbers. This means that in the initial phase of formation of the arms, the perturbed surface density of the gaseous disk $\tilde{\sigma}$ may be written

$$\tilde{\sigma} \;=\; C_\sigma(R, t)\;\cos[m\varphi - F_\sigma(R)]\,, \tag{5}$$

where C_σ and F_σ are the amplitude and phase of the density wave. The phase is independent of time, because the frame of reference we choose rotates with the angular velocity of the spiral pattern. The amplitude of the surface density grows with time due to instability. In the saturation stage, the growth becomes very weak, but observations show that the amplitude itself is high, so that the maximum density on the crest of the wave significantly exceeds the background density. Unlike the surface density $\tilde{\sigma}$, the amplitudes of the perturbed velocity components $\tilde{V}_r$, $\tilde{V}_\varphi$, and $\tilde{V}_z$ become saturated, remaining much less than the circular velocity of the gas. In other words, after becoming saturated, these components are stationary, monochromatic, small amplitude waves, and may be written:

$$\tilde{V}_r(R, \varphi) = C_r(R)\,\cos[m\varphi - F_r(R)]\,, \tag{6}$$

$$\tilde{V}_\varphi(R, \varphi) = C_\varphi(R)\,\cos[m\varphi - F_\varphi(R)]\,, \tag{7}$$

$$\tilde{V}_z(R, \varphi) = C_z(R)\,\cos[m\varphi - F_z(R)]\,. \tag{8}$$

Taking into account that $V_r(R, \varphi) = \tilde{V}_r(R, \varphi)$, $V_\varphi(R, \varphi) = V_{rot}(R) + \tilde{V}_\varphi(R, \varphi)$, $V_z(R, \varphi) = \tilde{V}_z(R, \varphi)$, where V_{rot} is the rotational velocity and substituting (6) – (8) in (4), we obtain the model representation of the line-of-sight velocity:

$$V^{mod}(R,\varphi) = V_s + \sin i\,[V_{rot}(R)\cos\varphi +$$
$$+ a_{m-1}(R)\cos(m-1)\varphi + b_{m-1}(R)\sin(m-1)\varphi +$$
$$+ a_m(R)\cos m\varphi + b_m(R)\sin m\varphi +$$
$$+ a_{m+1}(R)\cos(m+1)\varphi + b_{m+1}(R)\sin(m+1)\varphi], \quad (9)$$

where the Fourier coefficients related to the phases and amplitudes of the velocity components are:

$$a_{m-1} = \frac{C_r \sin F_r + C_\varphi \cos F_\varphi}{2}, \quad (10)$$

$$b_{m-1} = -\frac{C_r \cos F_r - C_\varphi \sin F_\varphi}{2}, \quad (11)$$

$$a_m = C_z \cos F_z \operatorname{ctg} i, \quad (12)$$

$$b_m = C_z \sin F_z \operatorname{ctg} i, \quad (13)$$

$$a_{m+1} = -\frac{C_r \sin F_r - C_\varphi \cos F_\varphi}{2}, \quad (14)$$

$$b_{m+1} = \frac{C_r \cos F_r + C_\varphi \sin F_\varphi}{2}. \quad (15)$$

Now, if $m > 2$, we can restore the velocity field of the galactic disk. Indeed, the zeroth Fourier harmonic gives us the systemic velocity of the galaxy, and the first cosine Fourier harmonic describes the rotation velocity. Then, Eqs. (10) – (15) make it possible to calculate the six unknown functions (the three amplitudes and three phases on the right-hand side) if the six Fourier coefficients of the line-of-sight velocity on the left-hand side of these equations are known.

For two-armed spirals, the system of equations becomes incomplete:

$$V_{rot} + \frac{C_r \sin F_r + C_\varphi \cos F_\varphi}{2} = a_1^{obs}, \quad (16)$$

$$- C_r \cos F_r + C_\varphi \sin F_\varphi = 2\,b_1^{obs}, \quad (17)$$

$$- C_r \sin F_r + C_\varphi \cos F_\varphi = 2\,a_3^{obs}, \quad (18)$$

$$C_r \cos F_r + C_\varphi \sin F_\varphi = 2\,b_3^{obs}, \quad (19)$$

To solve this problem, we propose to use some additional relations between velocity residuals, which follow from the wave nature of the disk perturbations. In general, we try two different approaches: starting from the expected relationships between the phases of the azimuthal and radial velocity components (the first method) and between the phases of the density and radial velocity perturbations (the second method).

For tightly-wound spirals $|\partial \ln f/\partial \ln R| \gg 1$ (note that this condition is much

less restrictive than the WKB approximation), the following relations between the phases of the radial and azimuthal velocity perturbations are valid outside the corotation radius (Lyakhovich et al. 1997):

$$F_\varphi(R) = F_r(R) \mp \pi/2\,, \quad \text{for} \quad \kappa^2 > 0\,, \tag{20}$$

$$F_\varphi(R) = F_r(R) \pm \pi/2\,, \quad \text{for} \quad \kappa^2 < 0\,. \tag{21}$$

Here and below, the upper and lower signs correspond to regions inside and outside the corotation radius, respectively, so that the relation between phases "switches over' at the corotation circle. The way in which this "switching" comes about can be different, however, and depends on the type of spiral (leading or trailing) and the direction of rotation of the disk in the pattern frame. For trailing spirals and $\kappa^2\Omega > 0$ (Lyakhovich et al. 1997):

$$F_\varphi(R_c) = F_r(R_c) + \pi\,, \tag{22}$$

while for $\kappa^2\Omega < 0$:

$$F_\varphi(R_c) = F_r(R_c)\,. \tag{23}$$

Taking into account (20), the system of Eqs. (16) – (19) may be written

$$V_{rot} = u_1^{obs} - \frac{1}{2}(C_r \perp C_\varphi)\sin F_r\,, \tag{24}$$

$$(C_r \pm C_\varphi)\cos F_r = -2\,b_1^{obs}\,, \tag{25}$$

$$(C_r \mp C_\varphi)\sin F_r = -2\,a_3^{obs}\,, \tag{26}$$

$$(C_r \mp C_\varphi)\cos F_r = 2\,b_3^{obs}\,. \tag{27}$$

This makes it possible to restore all parameters of the velocity field:

$$\operatorname{tg} F_r = -\operatorname{ctg} F_\varphi = -a_3^{obs}/b_3^{obs}\,, \tag{28}$$

$$\cos F_r = \operatorname{sign}\left(b_3^{obs} - b_1^{obs}\right)\sqrt{\frac{(b_3^{obs})^2}{(a_3^{obs})^2 + (b_3^{obs})^2}}\,, \tag{29}$$

$$C_r = (b_3^{obs} - b_1^{obs})/\cos F_r\,, \tag{30}$$

$$C_\varphi = \mp\,(b_3^{obs} + b_1^{obs})/\cos F_r\,, \tag{31}$$

$$V_{rot} = a_1^{obs} - \frac{a_3^{obs}\,b_1^{obs}}{b_3^{obs}}\,. \tag{32}$$

As before, the upper sign is for $R < R_c$ and the lower for $R > R_c$.

The amplitudes must always be positive, so that equations (30) and (31) are

consistent only if

$$\begin{array}{l} |b_3^{obs}(R)| - |b_1^{obs}(R)| \leq 0, \text{ for } \quad R < R_c, \\ |b_3^{obs}(R)| - |b_1^{obs}(R)| \geq 0, \text{ for } \quad R > R_c. \end{array} \tag{33}$$

This condition enables us to determine the approximate location of the corotation radius from the observational data.

As noted above, another way to complete the system of equations (16) – (19) is to use the relation between the phases of the density and radial velocity perturbations. It can be shown that if $|\mathrm{Im}\, k| \ll |\mathrm{Re}\, k|$, where k is the wave vector of the wave, these phases are related in a simple manner (Lyakhovich et al. 1997):

$$\begin{array}{lll} F_r(R) & = & F_\sigma(R) + \pi, \text{ for } R < R_c, \\ F_r(R) & = & F_\sigma(R), \quad\quad \text{for } R > R_c, \end{array} \tag{34}$$

and we have at the corotation radius:

$$F_r(R_c) = F_\sigma(R_c) - \pi/2, \text{for } \kappa^2\Omega > 0, \tag{35}$$

$$F_r(R_c) = F_\sigma(R_c) + \pi/2, \text{for } \kappa^2\Omega < 0. \tag{36}$$

The function $F_\sigma(R)$ is related to the observed shape of the spiral arms, and hence can be obtained from analysis of the second Fourier harmonic of the density (brightness) field. We then obtain from (34) and (16) – (19):

$$C_r = \mp \frac{b_3^{obs} - b_1^{obs}}{\cos F_\sigma}, \tag{37}$$

$$\mathrm{ctg}\, F_\varphi = \frac{2a_3^{obs} + (b_3^{obs} - b_1^{obs})\, \mathrm{tg}\, F_\sigma}{b_3^{obs} + b_1^{obs}}, \tag{38}$$

$$C_\varphi = \{(b_3^{obs} + b_1^{obs})^2 + [2a_3^{obs} + (b_3^{obs} - b_1^{obs})\, \mathrm{tg}\, F_\sigma]^2\}^{1/2}, \tag{39}$$

$$\sin F_\varphi = (b_1^{obs} + b_3^{obs})/C_\varphi \tag{40}$$

$$V_{rot} - a_1^{obs} - a_3^{obs} - (b_3^{obs} - b_1^{obs})\, \mathrm{tg}\, F_\sigma. \tag{41}$$

Relation (37) can also be used to find the location of the corotation radius:

$$\begin{array}{l} (b_3^{obs}(R) - b_1^{obs}(R))\, \cos F_\sigma(R) \leq 0, \quad \text{for } R < R_c, \\ (b_3^{obs}(R) - b_1^{obs}(R))\, \cos F_\sigma(R) \geq 0, \quad \text{for } R > R_c. \end{array} \tag{42}$$

6 Restoration of the velocity field in the galaxy NGC 157

NGC 157 is a rather nearby galaxy with a well-developed two-armed spiral structure. Unusual gas motions in the outer part of this galaxy were first noted in

long-slit observations by Zasov and Kyazumov (1981). The restoration of the vector velocity field of NGC 157 discussed below is based on observations at the 6-m telescope of the Special Astrophysical Observatory in 1995. The observations were carried out in the H_α line with a scanning Fabry-Perot interferometer and focal reducer at the prime focus of the telescope. A 512×512 two-dimensional photon-counting system operating in TRIM-mode was used as a detector. The data reduction (phase recalibration, flatfielding, velocity calculations, etc.) was done using the ADHOC software developed at the Marseille Observatory. As a result, we obtained a $256 \times 256 \times 32$ data cube with a spatial bin $0.92''$/px and spectral bin 19 km/s. The angular resolution was about $2.5''$ and the spectral resolution was 40–50 km/s. In general, more than 11,000 measurements of line-of-sight velocities were obtained over the disk of the galaxy. The best-fit parameters of the galactic disk of NGC 157 are: systemic velocity V_s — 1667 km/s, position angle of major dynamical axis $(PA)_o = 223.^\circ5$, and inclination angle i = - $51.^\circ5$ (the minus sign is the result of assuming that the spiral arms in the galaxy are trailing).

Our Fourier analysis showed that the first, second, and third harmonics clearly dominate in most parts of the disk. Superposition of the second and modified third harmonics on the H_α image of the galaxy is shown in Fig. 5. The good correspondence of the phase curves with the observed positions of spiral arms gives strong evidence that the non-circular velocities are associated with the spiral structure. This enables us to use the method described in the previous sections to restore the velocity field of this galaxy (see details in Fridman et al. 1997).

The two methods of velocity field restoration described above gave similar results. To construct the final velocity field model for the galaxy, we varied the radial dependence of the velocity residuals in the uncertainty range obtained by comparing the two methods for determining R_c. The best-fit model rotation curve is shown in Fig. 6. For comparison, the rotation curve obtained in a traditional way with a pure rotation model is also presented. Fig. 7 shows the behavior of $|b_2^{obs}(R)| - |b_1^{obs}(R)|$ in NGC 157. ¿From these data the corotation radius is found to be about $43'' \pm 3''$. Fig. 8 shows the dependence of $(b_3^{obs} - b_1^{obs}) \cos F_\sigma$ on galactocentric radius R. The estimate of R_c from Eq. (42) is $50'' \pm 1''$, in rough agreement with the value found from (33). Thus, we conclude that the corotation radius is within 40–$50''$. Note that a similar result ($50''$) was recently obtained in numerical simulations of NGC 157 by Sempere and Rozas (1997). Analysis of the variation of the phase difference between the radial and azimuthal perturbed velocities leads to the most reliable estimate of $R_c = 42''$; we use this value below for the best-fit model.

The restored velocity field in a reference frame rotating with the pattern speed obtained in the best-fit model is shown in Fig. 9. A similar procedure was applied to the spiral galaxy NGC 3893. The restored velocity field for this galaxy is presented in Fig. 10. We can clearly see that the velocity fields of both galaxies demonstrate two anticyclones located between the spiral arms near the corotation radii. The velocity amplitude of the vortices is about 30 km/s in both cases. In

addition, we can see that the directions of the velocity vector at the spiral arms are opposite on either side of the corotation circle. This result is in agreement with our main assumption about the wave nature of spiral structure.

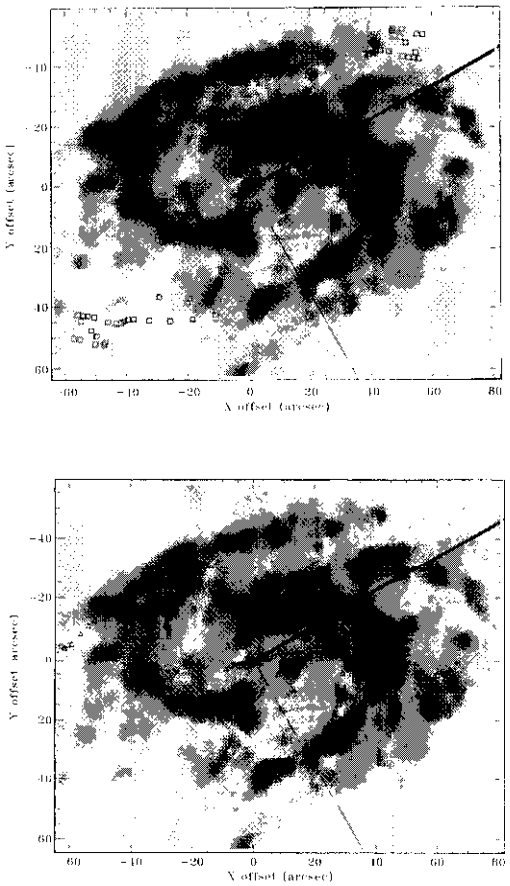

Fig. 5. Superposition of the second (up) and modified third (down) harmonics of the line-of-sight velocity field on the H_α image of the galaxy (gray scale). The modified third harmonic has the form $\cos(2\varphi + \pi/2 - F_3)$, where F_3 is the phase of the original third harmonic. The squares and triangles show the azimuth positions of the maxima of the harmonics at each radius. The good correspondence of these phase curves with the observed positions of the spiral arms gives strong evidence that the non-circular velocities are associated with the spiral structure.

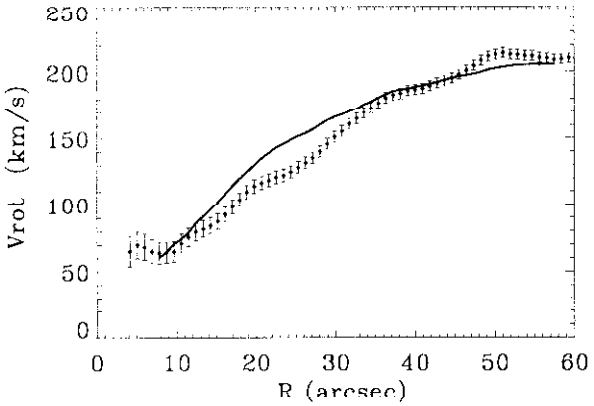

Fig. 6. Rotation curve of NGC 157 for the best-fit model (solid line) and in a pure-rotation model (dotted line with 3σ error bars).

7 Conclusions

1. The existence of dynamical formations, such as giant anticyclonic vortices, near the corotation radius was predicted on the basis of successful laboratory experiments with differentially rotating shallow water. This modeling was based on the equivalence of the dynamical equations for a galactic gaseous disk and for rotating shallow water.

2. Analysis of the velocity field of Mrk 1040 first demonstrated the presence of vortex structures in a real spiral galaxy.

3. Evidence for the presence of an anticyclone in the solar neighbourhood in the Galactic disk was obtained from an analysis of line-of-sight velocities of HII regions and young stellar objects.

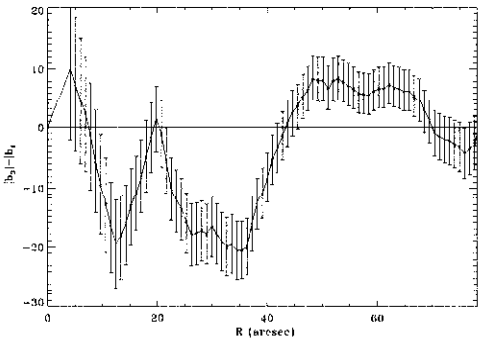

Fig. 7. Behavior of $|b_3^{obs}(R)| - |b_1^{obs}(R)|$ with galactocentric radius R in NGC 157. In the tightly-wound spiral approximation, this difference is negative inside the corotation radius and positive outside this radius. This approximation is not valid near the center and at the periphery of the galaxy. According to these data, the corotation radius is about $43'' \pm 3''$. Error bars correspond to 3σ.

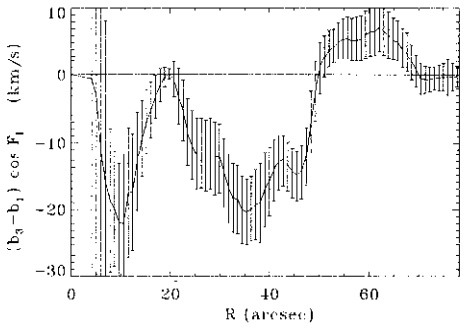

Fig. 8. Variation of $(b_3^{obs} - b_1^{obs}) \cos F_\sigma$ with galactocentric radius R in NGC 157. In the WKB approximation, the difference is negative inside the corotation radius and positive outside it. Error bars correspond to 3σ.

4. A method for restoring the full vector velocity field of a galaxy using observations of the line-of-sight velocity distribution of the gas has been developed. This makes it possible to determine the amplitudes and phases of gas perturbations related to density waves, and also to find the location of the corotation radius.

5. The velocity fields of several galaxies have been restored using this method, and the presence of giant anticyclones between spiral arms has been clearly demonstrated.

Our general conclusion is that the existence of vortex structures is *indeed a universal and observable property of galaxies* in which spiral arms are density waves.

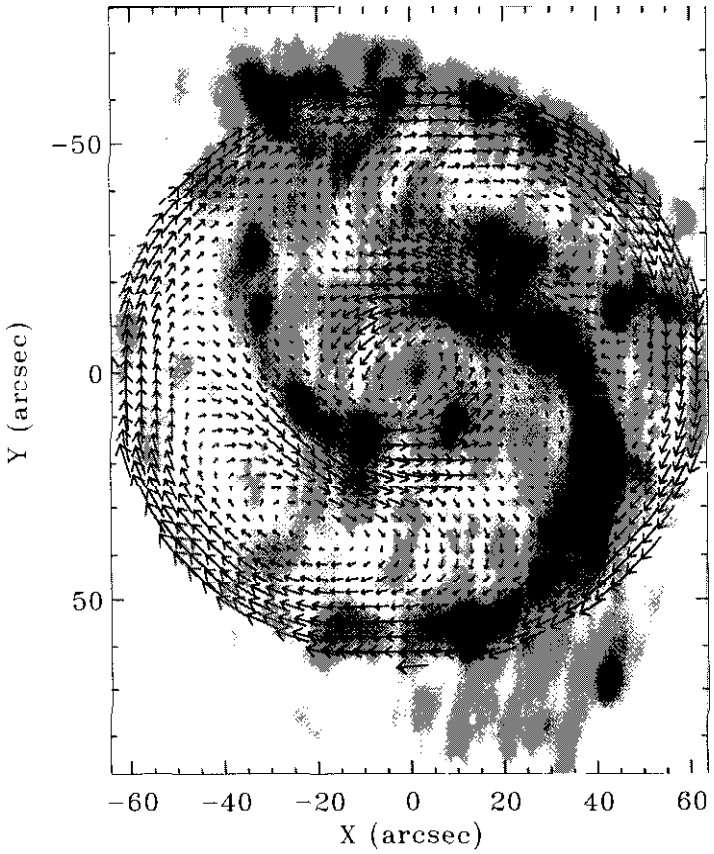

Fig. 9. Restored velocity field of NGC 157 in the reference frame rotating with the pattern speed overlaid on the H_α image of the galaxy.

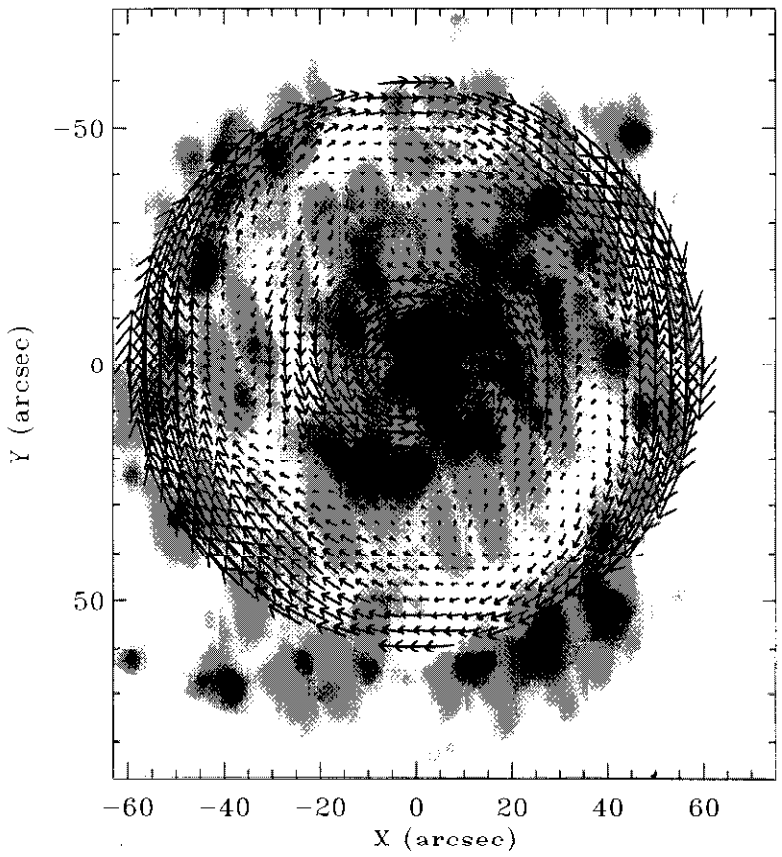

Fig. 10. Restored velocity field of NGC 3893 in the reference frame rotating with the pattern speed overlaid on the H_α image of the galaxy.

This work was partially supported by the Russian Foundation for Basic Research (grants N 96-02-17792, N 96-02-19636, N 96-02-18491) and a "Fundamental Space Research. Astronomy" grant for 1997.

References

Afanas'iev, V.L., Burenkov, A.N., Zasov, A.V., an Sil'chenko, O.K.: 1988, *Astrofizika*, **Vol. 28**, p. 243, **Vol. 29**, p. 155.

Afanas'iev, V.L. and Fridman, A.M.: 1993, *Pis'ma v Astron.Z.*, **Vol. 19**, p. 787.

Avedisova, V.S.: 1997, In press

Contopoulos, G.: 1978, *Astron. and Astrophys.* **Vol .64**, p.323.

Fridman A.M.: 1978, *Uspekhi Fiz Nauk* **Vol. 125**, p.352 & *Sov. Phys. Usp.* **Vol. 21**, p.536.

Fridman, A.M., Polyachenko, V.L.: 1984, *Physics of gravitating systems*. N.Y. etc.: Springer-Verlag, **Vol. 1**, **Vol. 2**.

Fridman, A.M., Morozov, A.G., Nezlin, M.V., Snezhkin, E.N.: 1985, *Phys. Lett.* A109, p.228.
Fridman A.M. 1990: In "Dynamics of Astrophysical Disks", Edited by J.A.Sellwood, Cambridge University Press, p.185.
Fridman A.M., 1994: In "Physics of the Gaseous and Stellar Disks of the Galaxy", Ed. I.R.King, PASP Conference Ser., V.66., P.15.
Fridman A.M., Khoruzhii O.V., Lyakhovich V.V., Avedisova V.S. 1996: Unsolved Problems of the Milky Way / eds. Blitz L. and Teuben P. Kluwer academic publishers, Netherlands, . P.597.
Fridman, A.M., Khoruzhii, O.V., Lyakhovich, V.V., Sil'chenko, O.K., Zasov, A.V., Rastorguev, A.S., Afanas'iev, V.L., Dodonov, S.N., Boulesteix, J., 1997 to be published.
Glushkova, E.V., Dambis, A.K., Mel'nic A.M., Rastorguev, A.S.: 1997, *Astron. Astrophys.* In press.
Lindblad, B.: 1941, *Stokholms Obs. Ann.* , **Vol. 29**, p. 155.
Lin, C.C., and Shu, F.H.: 1964, *Astrophys. J.*, **Vol. 140**, p. 646.
Lin, C.C., and Shu, F.H.: 1966, *Proc. Nat. Acad. Sci. USA*, **Vol. 55**, p. 229.
Lyakhovich V.V., Fridman A.M., Khoruzhii O.V.. 1996, *Soviet Astronomy Zh.*, **Vol. 73**, N1, p. 24.
Lyakhovich V.V., Fridman A.M., Khoruzhii O.V., Pavlov A.I.: 1997, *Soviet Astronomy Zh.*, **Vol. 74**, N4, p. 509.
Morozov, A.G., Nezlin, M.V., Snezhkin, E.N., Fridman, A.M.: 1984, *JETP Lett.*, **Vol. 39**, p.615.
Morozov, A.G., Nezlin, M.V., Snezhkin, E.N., Fridman, A.M.: 1985, *Sov. Phys. Uspekhi*, **Vol. 28**, p.101.
Nezlin, M.V., Polyachenko, V.L., Snezhkin, E.N., Trubnikov, A.S., Fridman, A.M.:1986, *Sov. Astron. Lett.*, **Vol. 12**, p.213.
Rastorguev, A.S.: 1997, *Astron. Astrophys.*. In press.
Sempere, M.J. and Rozas, M.: 1997,*Astron. Astrophys.*, **Vol. 317**, p. 405.
White,N.M. and Wing, R.F.: 1978, *Astrophys. J*, **Vol. 222**, p. 209.
Zasov A.V., Kyazumov H.A.: 1981, *Pis'ma v Astron.Z.*, **Vol. 7**, p. 131.